

LEADING EDGE RETRACTION AS A HIGH LIFT DEVICE

Robert F. Doss

Library
U. S. Naval Postgraduate School
Monterey, California

AIT	AIRFOIL
LIF	LIFT

LEADING EDGE RETRACTION
AS A HIGH LIFT DEVICE

8854

DCSS

1955

THESIS
D663

sis by

F. Doss

United States Navy

Letter on cover:

LEADING EDGE RETRACTION AS A HIGH
LIFT DEVICE

Robert F. Doss

of the Requirements

ree of

Aeronautical Engineer

California Institute of Technology

Pasadena, California

1955

Thesis by
Robert F. Doss
Lieutenant, United States Navy

In Partial Fulfillment of the Requirements
For the Degree of
Aeronautical Engineer

California Institute of Technology
Pasadena, California

1955

Thesis

D663

ACKNOWLEDGEMENTS

The author wishes to express his appreciation to Dr. H. J. Stewart and Dr. Anatol Roshko for their interest and guidance, and to his co-worker in most of the investigation, Lt. Carl Birdwell, USN, for his excellent assistance.

Library
Naval Postgraduate
Monterey, California

SUMMARY

A two-dimensional investigation was carried out in the Merrill Wind Tunnel at the California Institute of Technology to determine the effect on low speed lift of retracting the leading edge of a thin, circular-arc airfoil.

Several configurations were tried, some with a spanwise slot milled into the upper surface so that the leading edge recess formed by retraction could be utilized as an air intake to improve the flow. A comparison was made between the configurations with the leading edge retracted to various positions and the basic airfoil.

The investigation showed that leading edge retraction caused a linear loss of maximum lift proportional to the percent reduction in chord up to a critical position where lift and the stalling angle of attack increased abruptly. Thereafter, maximum lift was reduced at a rate higher than the chord reduction. The effect of the slot was negligible.

The critical position phenomena warrants further study.

TABLE OF CONTENTS

Part	Title	Page
	Acknowledgments	i
	Summary	ii
	Table of Contents	iii
	List of Figures	iv
	List of Symbols	vi
I.	Introduction	
II.	Apparatus	3
III.	Experimental Procedure	7
IV.	Results and Discussion	9
V.	Conclusions and Recommendations	16
	References	17
	Table I	18
	Figures	19

LIST OF FIGURES

Figure	Title	Page
1	Model Components and Leading Edge Positions	19
2	Partial Sectional View of Model Leading Edge	20
3	Slot Configurations	21
4	Model and Balance System	22
5	End View of Model in Test Section	23
6	Three-quarter View of Model in Test Section	23
7	Balance System Modification	24
8	Pressure Survey Probe Set-up	24
9	Static Pressure Probe and Set-up	25
10	The Effect of Leading Edge Retraction on Maximum Lift for Configuration 1a2	26
11	The Effect of Leading Edge Retraction on Maximum Lift for Configuration 1d2	27
12	The Effect of Leading Edge Retraction on Maximum Lift for Configuration 1d3	28
13	The Effect of Leading Edge Retraction on Maximum Lift for Configuration 23	29
14	C_{l10} vs. α for Configuration 1a1	30
15	C_{l10} vs. α for Configuration 1a2	31
16	C_{l10} vs. α for Configuration 1b2	32
17	C_{l10} vs. α for Configuration 1d2	33
18	C_{l10} vs. α for Configuration 1d3	34
19	C_{l10} vs. α for Configuration 23	35
20	Slot Effectiveness for Configurations 1d3-0 and 1d3-4	36
21	Slot Effectiveness for Configurations 1c2-0 and 1c2-4	37
22	Probe Tuft Survey Sketch for Configuration 1d3-4	38

LIST OF FIGURES (Continued)

Figure	Title	Page
23	The Effect of Angle of Attack on Pressure Distribution of Configuration 1d3-4	39
24	The Effect of Leading Edge Retraction on the Upper Surface Pressure Distribution of Configuration 1c2 at $\alpha = 10^\circ$	40
25	Vortex Hypothesis	41
26	The Effect of Slot Size and Configuration at the Fully Retracted Position	42

LIST OF SYMBOLS

C_l	-	section lift coefficient
$C_{l_{10}}$	-	section lift coefficient based on 10 inch chord
C_{l_x}	-	section lift coefficient based on actual chord
$C_{l_{max}}$	-	maximum section lift coefficient
α	-	angle of attack
α_s	-	angle of attack at stall
C_{pu}	-	pressure coefficient, upper surface

I. INTRODUCTION

Sharp leading-edged, thin airfoils have poor low speed characteristics, particularly maximum lift coefficient. Recently these airfoils have been introduced to advance the supersonic capabilities of fighter aircraft. In order to approach reasonable landing speeds the airfoils have had to be modified to incorporate high lift devices such as nose flaps, slats or boundary layer control. These devices have several disadvantages. Nose flaps and slats on thin airfoils must employ partially external actuators to provide and support the moment during low speed operation, but during high speed flight the actuators contribute considerably to drag. Boundary layer control is usually dependent on engine operation. Supersonic aircraft should have a "dead stick" landing capability to take advantage of the excellent glide ratio and the usual high altitude and high speed of operation. Boundary layer control further imposes a constraint, though of less importance, on engine performance in that maximum thrust cannot be developed at both the high lift and high speed configurations. The disadvantages of presently employed devices prompted this investigation into the potentialities of leading edge retraction, a mechanically simple operation.

Thin airfoil stall is characterized by a separated region or "bubble" at the leading edge which grows chordwise with increasing angle of attack until it reaches the trailing edge and the wing stalls (Ref. 1). The separation at the leading edge is caused by the inability of the flow to negotiate the very small nose radius. The mechanism of reattachment of the flow is not fully understood (Ref. 1), but it seems logical that the flow is aided by a vortex pattern which appears within the bubble.

It occurred to the author that by retracting a small portion of the

leading edge the flow might be turned from the stagnation point to the upper surface in stages. Interaction between the edges formed by the retraction might simulate a greater nose radius and cause a delay in stall. Another possibility of flow improvement at high angle of attack might exist in retracting the leading edge within the wing to form an air intake for re-energizing the confused flow within the bubble. The obvious disadvantage to leading edge retraction is the loss in wing area. Therefore, to make a significant contribution to low speed lift the retraction must increase the lift coefficient based on the original chord.

The investigation was conducted in the Merrill Wind Tunnel of the Guggenheim Aeronautical Laboratory at the California Institute of Technology during March and April, 1955.

II. APPARATUS

The tests were conducted in the Merrill Wind Tunnel, a closed-circuit type with a 32 by 45 inch test section and a 6:1 contraction ratio. Power was supplied by a 75 H.P. constant speed electric motor driving a three-bladed electric pitch controlled propeller giving a speed range of 0 to 180 mph. During the tests there were three 32-mesh wire screens mounted at the entrance to the contracting section to decrease turbulence.

The model tested was a circular arc 6 percent thick airfoil of 10 inch chord and 24 inch span. The model was fabricated from full span components in order to permit various configurations. The components were contoured from brass on a horizontal planer and hand finished with a file and fine emery paper. The base of the model consisted of the aft 50 percent of chord and a tongue. The various configurations were achieved by bolting upper and lower contoured sections to the tongue, leaving a space for retracting the leading edge. The first configuration provided the largest recess. Thereafter, the configurations restricted the recess more each time and the leading edge piece was then milled in thickness to fit. This method prevented retesting a configuration after an alteration had been made but it permitted several configurations with only one leading edge piece, saving considerable time and money. Figures 1 and 2 show sectional views of the components. Significant chordwise dimensions are listed in Table I.

A spanwise slot was incorporated in one upper-surface section. The slot was maintained by eight 0.0625 inch brass fingers which were secured in milled recesses in the fore piece by solder. The fingers were secured to simultaneously cut recesses in the main piece by glyptol glue. The slot

was altered in shape once and in size several times during the tests (Fig. 3). The size change was achieved by shifting the upper leading edge out or in. This changed the upper chord about 0.010 inches, but the effect on curvature was negligible.

The model configurations were designated by a four-digit descriptive number as follows: (top piece) (slot configuration, if any) (bottom piece) dash (leading edge position). There were two top pieces, numbers 1 and 2, and three bottom pieces, numbers 1, 2, and 3. Top piece number 1 had four slot configurations: a, b, c, and d. The leading edge positions were described by numbers 0 through 7, by a position called "flush" which indicated when the leading edge was flush with the top piece edge, and by a position called "basic" which was the fully extended position making up the basic circular-arc airfoil. Intermediate positions were described by hundredths of the space between the numbers, i.e.---leading edge position half way between 4 and 5: 4.50. In all configurations the top piece extended ahead of the bottom piece and hence the top piece defined the chord when the leading edge was retracted beyond the flush position.

Circular end-plates 15 inches in diameter were secured to the base piece. The outer edges were beveled 15 degrees to decrease the influence of the end plates on the model. The inner faces ahead of the base piece were milled to receive the ends of the retractable leading edge. A .125 inch wide slot was milled into each receiver so that two .125 inch locking bolts tapped into each end of the leading edge piece could ride during retraction. The leading edge was fixed into the various positions by tightening the locking bolts. The positions were indicated by marking the end plates at approximately every $1/4$ inch and using the base end of the leading edge piece as a reference.

The model was mounted on a three point support in the wind tunnel. There were two forward struts which connected to trunion pins at the 50 percent chord point on the model outboard of the end plates. The tail support connected to a 1/2 inch diameter spanwise rod joined on each end to 12 inch tail stings mounted on the end plates. The three supports went through the test section floor to connect with the balance system. Figure 4 shows the model and balance system. Figures 5 and 6 show the model in the test section with leading edge retracted to position 4.

The balance was modified to support the severe dynamic loads imposed by the model at stall (Fig. 7). A 1/2 x 1 x 8 inch bar was connected at the tail support pivot to the angle of attack setting moment arm. A similar bar was connected to a gusset on the inner lift frame. The free ends of the bars were connected by a wide-flange sheet metal clamp secured by two bolts and wing nuts. After the angle of attack was set, the clamp was tightened to permit the rigidity of the lift frame to damp the oscillation of the relatively weak balance moment arm.

Static measurements showed the lift balance to be accurate to $\pm .01$ pounds. Accuracy of results is discussed in section IV.

Besides force measurements upper surface pressure and tuft surveys were made. The pressure surveys were conducted with a static pressure probe made from .032 inch O.D. stainless steel tubing. To minimize the effect of orientation and yaw, three evenly spaced No. 80 holes were drilled circumferentially .75 inches from the nose of the probe. Fine piano wire (.012" dia.) was soldered into the front end of the probe and extended forward in the tunnel through a small grommet attached to an upper hanger made of the same wire and out the bottom on the tunnel just ahead of the test section. The probe was 13 inches long. A rubber hose and another fine wire were attached to the rear of the probe at an expanding section. The

hose and wire passed through a nylon housing which was secured to the aft model support. The nylon housing carried the hose outside the test section. The pressure was measured on an alcohol micromanometer referenced to stream static pressure. The probe was adjusted by the fore and aft wires. The upper hanger was used to support the fore wire tangent to the leading edge, requiring adjustment with change in angle of attack. The probe positions were identified by 1/2" marks numbered 0 through 20 on the wing starting at the trailing edge with 0. A stripe of bluing behind the static holes on the probe aided their alignment with the marks of the wing. The survey was accomplished nose to tail without interruption, the only delay being caused by the time lag in pressure stabilization due to the damping of the small tube. Figures 8 and 9 show the probe and set-up.

The tuft surveys were carried out with a probe made from 1/4 inch drill rod, tapered and fitted at one end with .032 inch stainless steel tubing. A single strand of cotton thread 3/8 inches long was inserted and glued into the tube.

III. EXPERIMENTAL PROCEDURE

Much of the testing of the model was carried out jointly with another investigator (Ref. 2). Lift measurements were made for all of the model configurations; drag measurements were made for some configurations. The balance modification precluded any moment measurements. Since this report is concerned with the effect of leading edge retraction on lift only, no further reference will be made to the drag measurements.

Lift data was measured directly by the balance system and corrected by an aerodynamic tare taken with the model removed from the endplates and supports. No wind tunnel boundary corrections were made. The tare was run at a dynamic pressure, q , of 20 lbs./ft.². All other runs were made at $q = 25$ lbs./ft.². The Reynolds number based on a 10 inch chord was 710,000. The lift measurements were converted to coefficient form and plotted during each run so that questionable points or observed phenomena could be double-checked. The basic 10 inch chord was assumed for all configurations and leading edge positions in converting to lift coefficient so that realistic comparison could be made between the configurations and the unaltered airfoil. A record of the repeatability of the data was kept in order to determine the experimental error.

A basic airfoil configuration was run after each modification to the model. On the initial basic configuration test, the leading edge piece junctures with the upper and lower components were covered with scotch tape to minimize any effect of some sharp edge irregularities. Repeating the run with the scotch tape removed showed the tape to have no noticeable effect. Scotch tape was also utilized to cover the various spanwise slots. Comparing these runs with the open-slot runs enabled the slot effectiveness

to be determined. Runs during which tape was employed are designated by (ts) at the end of the configuration number.

The leading edge was retracted from the basic position step by step to the fully retracted position. At each step force measurements were made, usually over a range of angle of attack from -2 to 14 degrees. Several times the range of angle of attack was limited to the upper portion of the lift curve.

Pressure and tuft surveys were made over the upper surface of some configurations in an effort to describe variations in lift measurements between leading edge positions. The model was set at the desired angle of attack and a survey accomplished. The angle of attack was then altered, and in the case of the pressure survey the probe was re-aligned to travel tangent to the model surface. The run was repeated. The tuft survey was conducted by positioning the tuft with the probe, observing the action, and sketching it. The tunnel speed for the surveys was the same as for the force measurements.

IV. RESULTS AND DISCUSSION

The lift measurements as determined by repeatability were accurate to $\pm .04$ pounds, equivalent in lift coefficient to $\pm .001$, up to the stalling angle of attack. In the immediate vicinity of the stalling angle the lift measurements were accurate to $\pm .12$ pounds, and at higher angles the accuracy was $\pm .20$ pounds.

The most important observation in the investigation was the occurrence of a favorable but critical leading edge position (Figs. 10-13). Note in particular Figure 12. Retracting the leading edge caused a decrease in the maximum lift coefficient based on the original chord up to a certain position defined here as the critical position. At this point, $C_{l_{max}}$ made an abrupt increase to equal or exceed the basic maximum lift coefficient. Further retraction caused an abrupt decrease in $C_{l_{max}}$ with the least $C_{l_{max}}$ occurring in most cases where the upper edge and leading edge were in the same vertical plane. Retraction within the wing had only a slight effect over the already reduced $C_{l_{max}}$. This behavior suggests three regions for discussion: (1) the positions before critical, (2) the critical position, and (3) the positions after critical where the leading edge is fully within the wing.

(A). Before critical.

The reduction of lift due to retraction of the leading edge from the basic position to a position approximately one percent of chord from the flush position was linear. Correcting the lift coefficient for reduction in chord produced a constant coefficient for this region showing that the reduction was due entirely to loss in wing area (Figs. 10, 12, and 13). The upper portions of the lift curves for all configurations are shown in Figures 14 through 19. Com-

paring the different configurations at positions 5 and 6 showed no significant effect due to configuration. Throughout this region the nose piece was not retracted sufficiently to open the slot.

(B). The critical position.

As the leading edge was retracted to the vicinity of the upper edge, lift abruptly increased. Retraction in this region over a range of less than one percent chord caused a change from the low, chord reduced lift coefficient to a maximum lift coefficient, followed by a decrease to a minimum lift coefficient. The stalling angle of attack was 10 degrees for every position except the critical where it was 12 degrees. The slope of the lift curve for the critical position was less than the slope of the lift curve for the basic airfoil.

The critical position was not achieved for every configuration because of the extreme sensitivity of the position. The first configuration tested was configuration 1a1 (Fig. 14). At position 4 the lift increased substantially and α increased to 12 degrees. The second configuration when tested at position 4 showed only a slight increase in lift (Fig. 15). The third configuration showed no increase. The other tests were similarly inconsistent at position 4. The results were further confused when scotch tape was placed over the slots and the tests were repeated showing in some cases the lift to be higher and in some cases the lift to be lower. When the maximum lift coefficients for all configurations at position 4 were plotted, the curves showed a variation of nearly 30 percent of the basic lift coefficient. This inconsistency pointed to the high sensitivity of position.

The model was re-assembled in configuration 1d2 and carefully tested in the critical region (Fig. 17). Variations of .005 inch in

retraction produced considerable change in maximum lift coefficient (Fig. 11). This .005 inch variation was much less than the positioning error and explained the inconsistency first noted. In fact, the model leading edge accuracy when compared to a spanwise straight-edge showed a variation of $\pm .020$ inches. The critical position was located by trial and error; and, when maximum lift was obtained, the position was called 4.00. Configuration 1d3 was then carefully tested and the critical position achieved (Figs. 12 and 18). Prior to assembling and testing configuration 23, the leading edges were worked over and the straight-edge variation was decreased to $- .010$ inches.

The slot effect in the critical region was negligible. Figure 20 shows the comparison of 1d3-4 and 1d3-4(ts) where the critical position was achieved, and Figure 21 shows the comparison of 1c2-4 and 1c2-4(ts) where the critical position was not quite achieved. The tuft surveys for these configurations showed the flow to be up-stream on the surface of the wing in the vicinity of the slot (Fig. 22). In one case the tuft was sucked into the slot from the upper surface but the suction was very weak. The tuft could usually be made to lie across the slot or in it at will, pointed in the up-wind direction.

The slot and taped slot configurations of 1d3-4 at the stalling angle of attack were compared by pressure surveys. As is shown in Figure 23 the slot effect was to decrease the absolute magnitude of pressure over the first 15 percent of the upper surface and to slightly increase it over the remainder of the wing. The net effect was a zero change in lift. The small change in pressure distribution would probably have a very slight effect on drag and pitching moment. Figure 24 shows a similar slot effect. The small pressure peaks occur-

ring 82.5 percent from trailing edge are caused by the influence of the slot on the probe. Flow here was not always parallel to the static orifices causing a dynamic component of pressure to be picked up.

The mechanism for the achievement of higher lift and later stall is not known. It is suggested, however, that at the critical position a vortex forms between the leading edge and upper edge and permits the flow to attack the upper edge at an angle more favorable for negotiation than if a stagnation point existed. Sketches in Figure 25 illustrate the hypothesis. The supposition of an aiding vortex is advanced by a test on configuration 1d2-4 where scotch tape was used to cover the three edges to form a triangular shaped nose (Fig. 17). The tape prevented the action of the supposed aiding vortex and the resulting lift was considerably less than the non-taped critical position lift. The stalling angle of attack of the taped-edge configuration was 10 degrees whereas the stalling angle of attack of the non-taped configuration was 12 degrees. The taped-edge configuration lift curve resembled the curves of the configurations on either side of the critical position.

An attempt was made to more clearly define the critical position. The angle formed with the chord line by a line connecting the leading edge and the upper edge was measured. Because of the spanwise irregularities this angle varied considerably. The angle was determined from the average of several measurements made at different spanwise stations to be 59 degrees. Probably the critical position was not achieved everywhere at the same leading edge setting because of this spanwise irregularity.

An opportunity to evaluate the scale effect on the critical position occurred between configurations 1d3 and 23. The increment of $C_{l_{max}}$ between the basic position and the critical position when corrected for decrease in chord was .077 for configuration 1d3 and .044 for configuration 23. The critical angle was approximately the same in each configuration, but the vertical distance between the edges was less for configuration 23 than for configuration 1d3. The ratio of vertical distances was determined from the data in Table I to be 0.58. The ratio of $\Delta C_{l_{max}}$ was 0.57. These ratios indicated a linear increase in $C_{l_{max}}$ with an increase in scale. A further pursuit of similarity could not be made because the governing parameters were not all known.

(C). After critical.

Retraction of the leading edge into the wing was to provide an intake for air to re-energize the flow in the bubble and thereby aid flow re-attachment and delay stall.

The method was ineffective as is shown in Figures 10 and 12. In no configuration of this region did the maximum lift coefficient increase above the chord-reduced coefficient. In configuration 1a2 the fully retracted position produced a slightly higher $C_{l_{max}}$ than the flush or intermediate positions (Fig. 10). In configuration 1d3 the flush position was higher (Fig. 12).

The effect of the slot for the fully retracted position is illustrated in Figures 20 and 21. For configuration 1d3-0 the slot caused an earlier stall than for the taped-slot. The taped-slot lift curve slope was not linear, whereas the slope of the slot lift curve was linear. Figure 24 shows the pressure distribution for configurations 1c2-0 and 1c2-0(ts). The effect of the slot was opposite to that

of position 4 previously described. The slot caused a negative pressure peak over the area ahead of it which was about 70 percent higher than the pressure of the taped-slot configuration. If a substantial pressure recovery could be gotten by the intake, this pressure peak could probably be increased sufficiently to cause a significant increase in lift. The required pressure recovery was not possible with the configurations tried because the stagnation point was below the lower leading edge at high angles of attack.

A comparison of the effects of the various slots and configurations with the leading edge fully retracted is shown in Figure 26. The poorest configuration was 1b2-0 where the slot gap was the greatest. The best configurations were 1c2-0, 1c2-0(ms), and 1a2-0. Slots a and c were the same size, but smaller than slot b. The configuration 1c2-(ms) is shown in Figure 21. It was an intake modification made in an attempt to improve the flow, but very little difference in lift was noted.

To summarize, leading edge retraction from the basic airfoil configuration to the fully retracted position produced three distinct regions of interest. The first was the region of initial retraction where the lift decreased in proportion to the chord. The second was the region where the leading edge and upper edge interacted. Favorable interaction occurred at the critical position, causing a 2 degree increase in the stalling angle of attack and an increase in lift coefficient. The slope of the lift curve for the critical position was less than the slope of the lift curve for the basic configuration. The third region was the range of position where the leading edge was retracted past the flush position. The air intake and slot were ineffective in producing a significant increase in

lift because the pressure recovery was very small.

The effect of the lower edge was insignificant in the configurations tested. However, in view of the critical position phenomena, there may be a benefit realized by having the lower edge in a forward stagger position. To investigate this both the lower edge and leading edge must be movable.

The possibility of using leading edge retraction as a high lift device is indicated by the results. The lift increase achieved here was not in itself sufficient, but the indication of an increase in lift with an increase in scale leads to the possibility that a substantial lift increase may be gained with a very small chord retraction.

V. CONCLUSIONS AND RECOMMENDATIONS

The following conclusions can be drawn from the investigation on the effect of leading edge retraction on low speed lift of a 6 percent thick circular-arc airfoil:

1. Retraction of the leading edge caused an advantageous flow phenomenon at a critical position which warrants further study.
2. Retraction of the leading edge past the critical position was disadvantageous. The use of the space as an intake at high angles of attack was not satisfactory.
3. The slot did not significantly improve lift for the fully retracted leading edge. It was ineffective at the critical position.

It is recommended that the investigation of the critical position phenomenon be continued. Larger scale tests with accurate positioning devices for the lower and leading edges would be advisable.

REFERENCES

1. McCullough, G.B. and Gault, D.E.: "Examples of Three Representative Types of Airfoil-Section Stall at Low Speed", NACA TN 2502, 1951.
2. Birdwell, Lt. Carl, USN; "Investigation at Low Speed of a Six-percent Thick Symmetrical Circular-Arc Airfoil with Leading Edge Retraction in Combination with Nose Slot", AeE Thesis, Calif. Institute of Tech., 1955.

TABLE I

SIGNIFICANT DIMENSIONS FOR VARIOUS CONFIGURATIONS

Leading Edge Position (number)	Configurations (defined by top piece)	Chord (inches)	Leading Edge Position (inches from trailing edge)	Percent Retraction (of basic chord)
basic	1a,1b,1c,1d	10.000	10.000	0
7	1a,1b,1c,1d	9.867	9.867	1.33
basic	2	9.840	9.840	0
6	1a,1b,1c,1d	9.617	9.617	3.83
6	2	9.617	9.617	2.25
5	1a,1b,1c,1d	9.367	9.367	6.33
5	2	9.367	9.367	4.72
flush	2	9.285	9.285	5.65
4	2	9.285	9.100	
4	1a,1b,1c,1d	9.100	9.100	9.00
flush	1b	9.060	9.060	9.40
flush	1a,1c	9.040	9.040	9.60
flush	1d	9.030	9.030	9.70
3			8.850	
2			8.600	
1			8.350	
0			8.100	

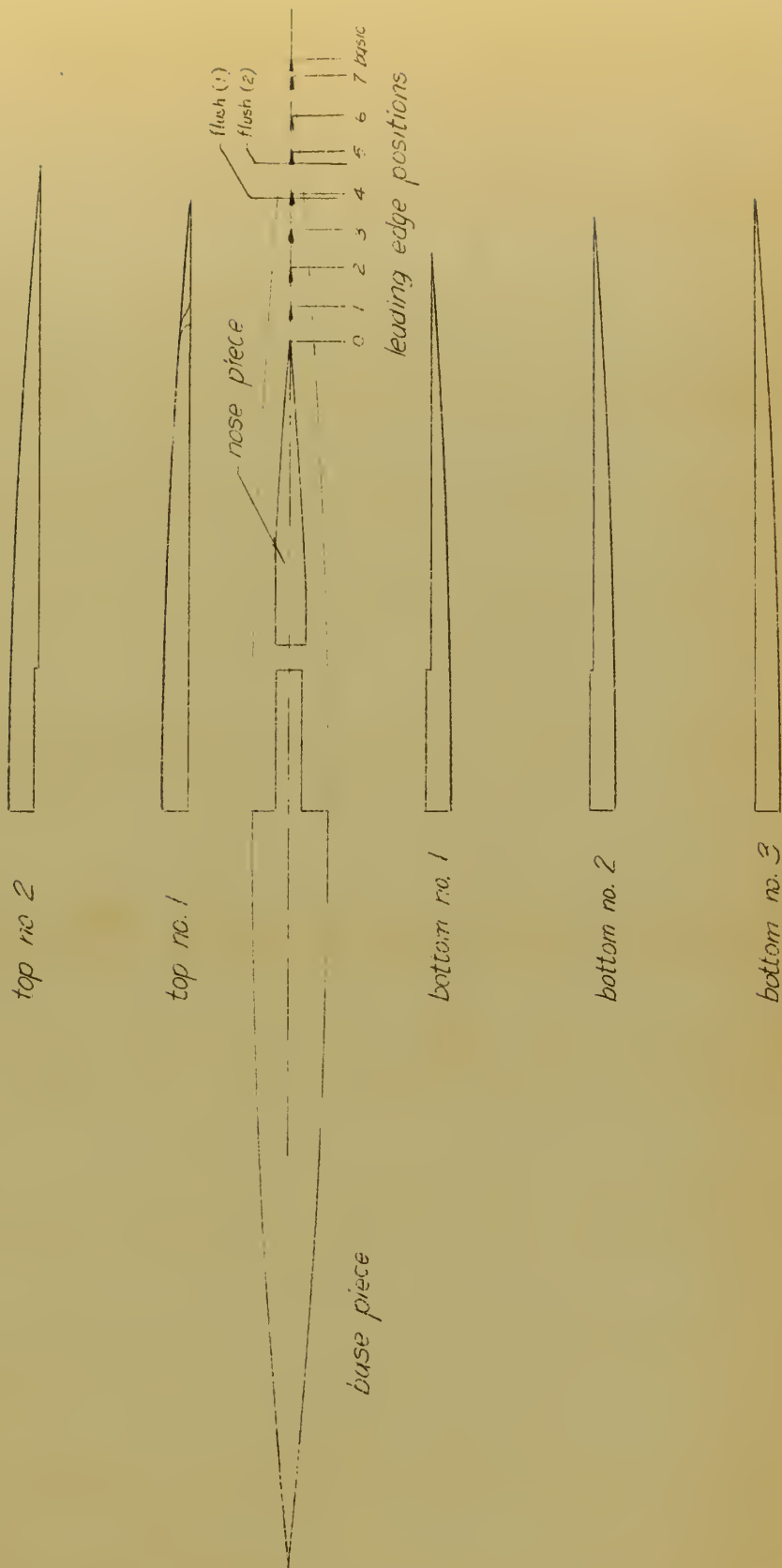


Fig. 1 Model Components and Leading Edge Positions

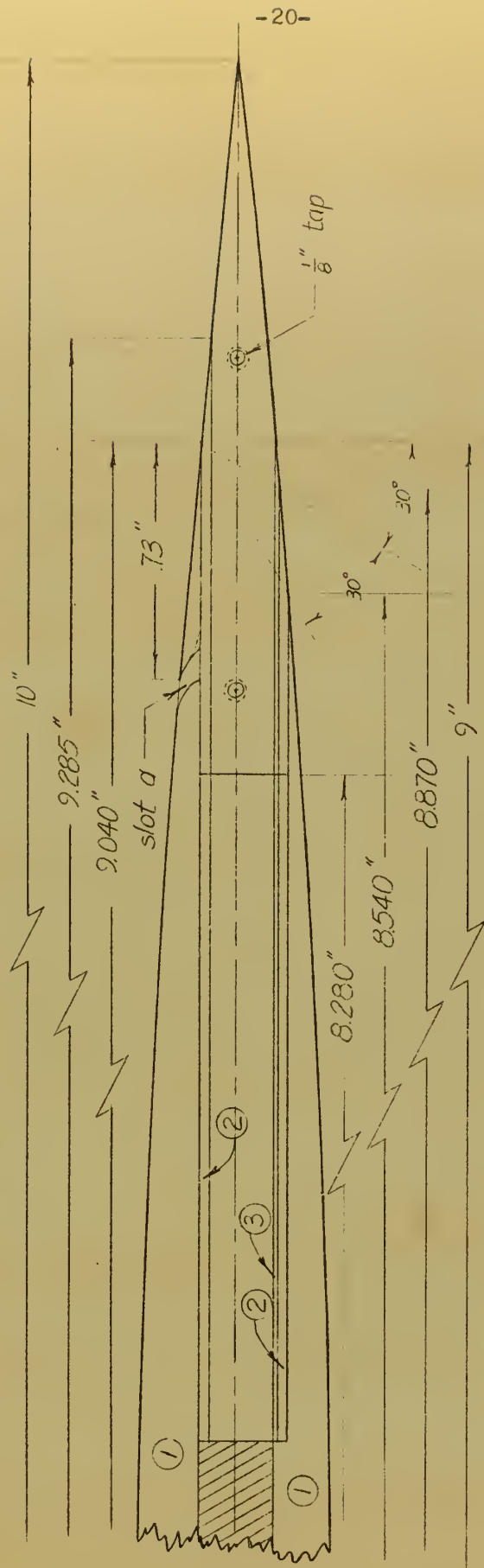
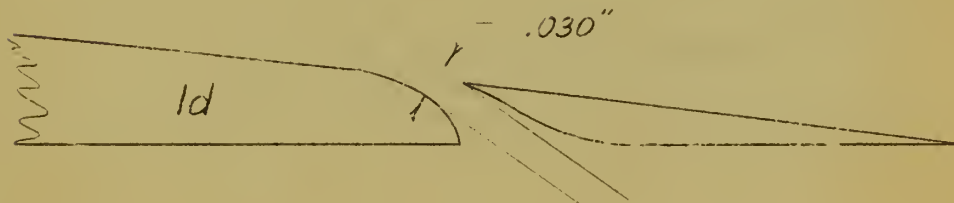
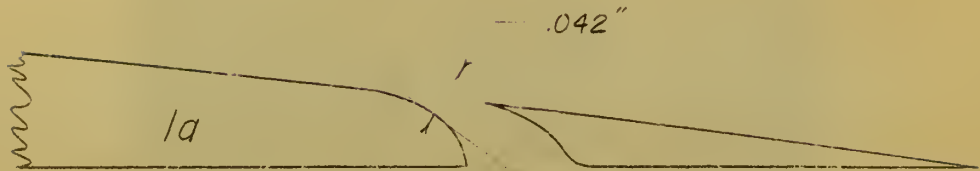


Fig. 2 Partial Sectional View of Model Leading Edge

Fig 3 Slot Configurations



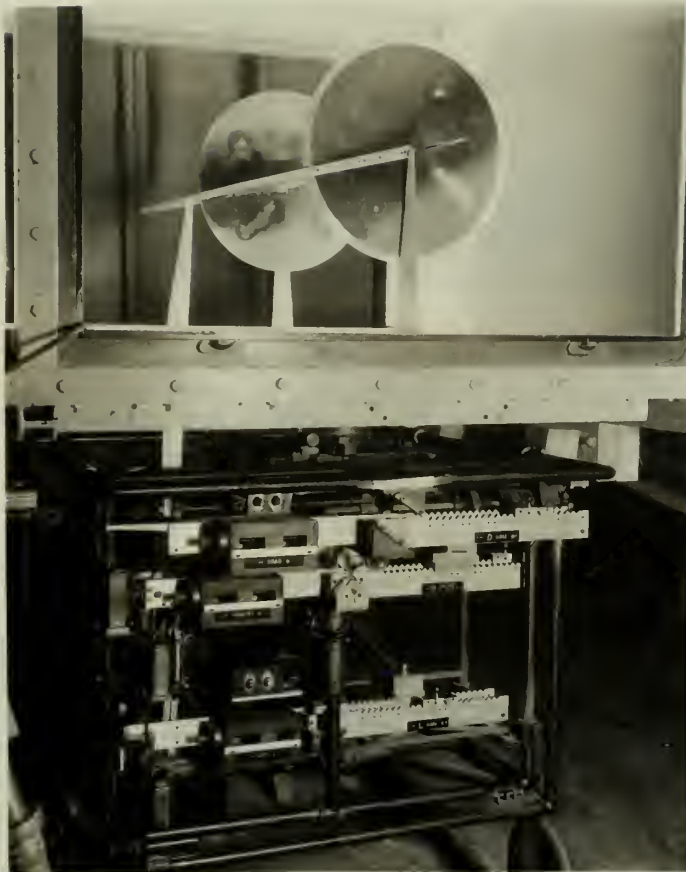


Fig. 4 Model and Balance System.



Fig. 5 End View of Model in Test Section,
End Plate Removed. Leading Edge at
Position 4.

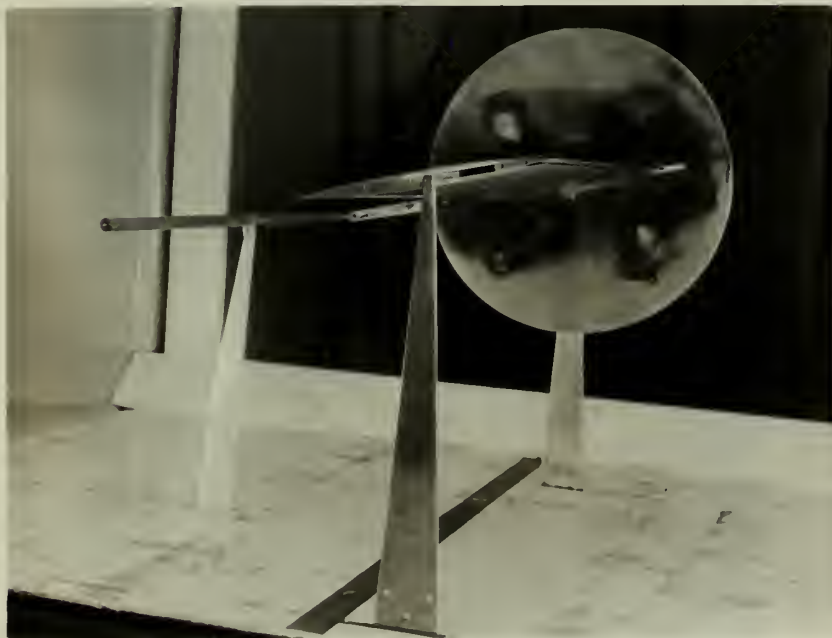


Fig. 6 Three-quarter View of Model in
Test Section.

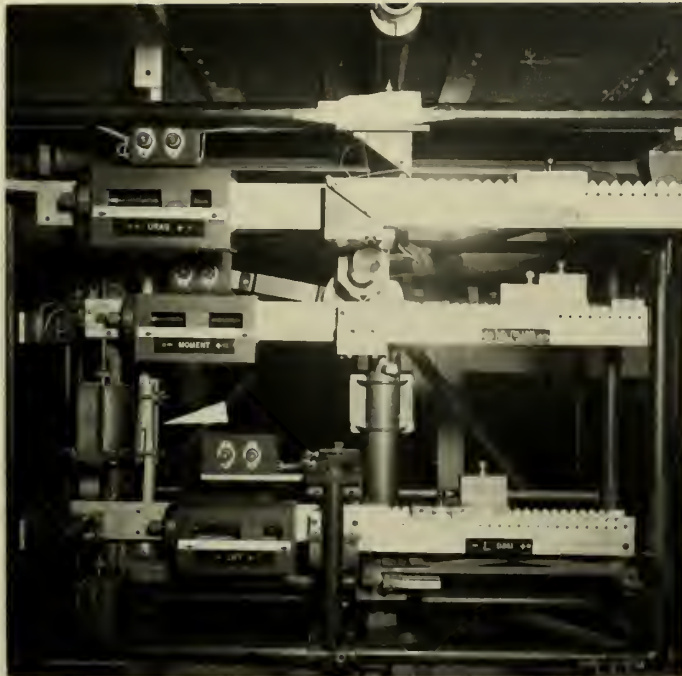
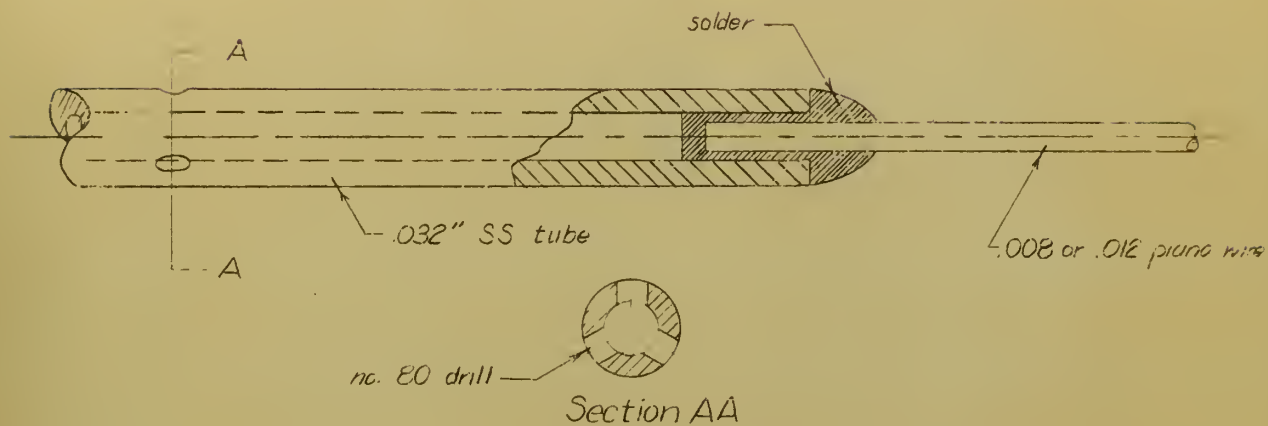


Fig. 7 Balance System Modification (Arrow).

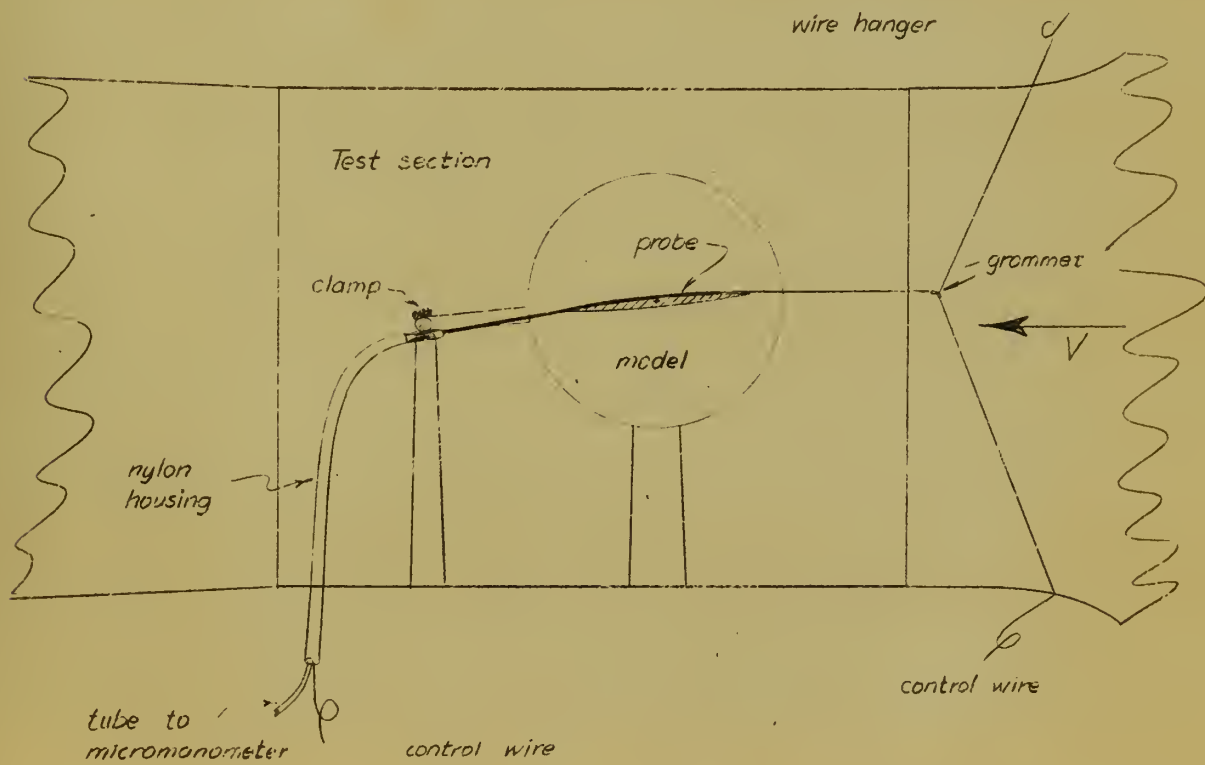


Fig. 8 Pressure Survey Probe Set-up.

Fig. 9. STATIC PRESSURE PROBE AND SET-UP



Probe



Set-up

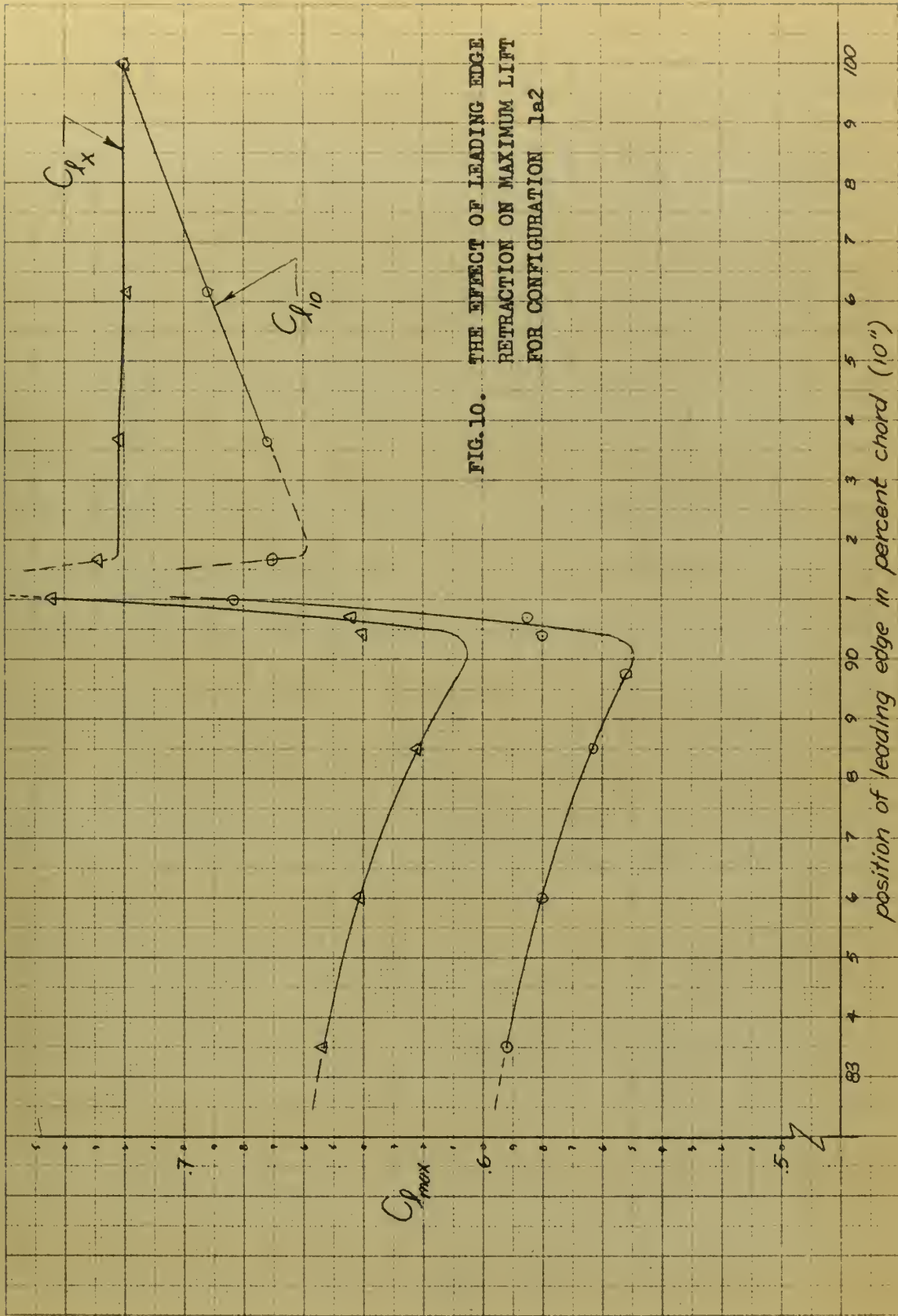


FIG. 11. THE EFFECT OF LEADING EDGE RETRACTION ON
MAXIMUM LIFT FOR CONFIGURATION 1d2

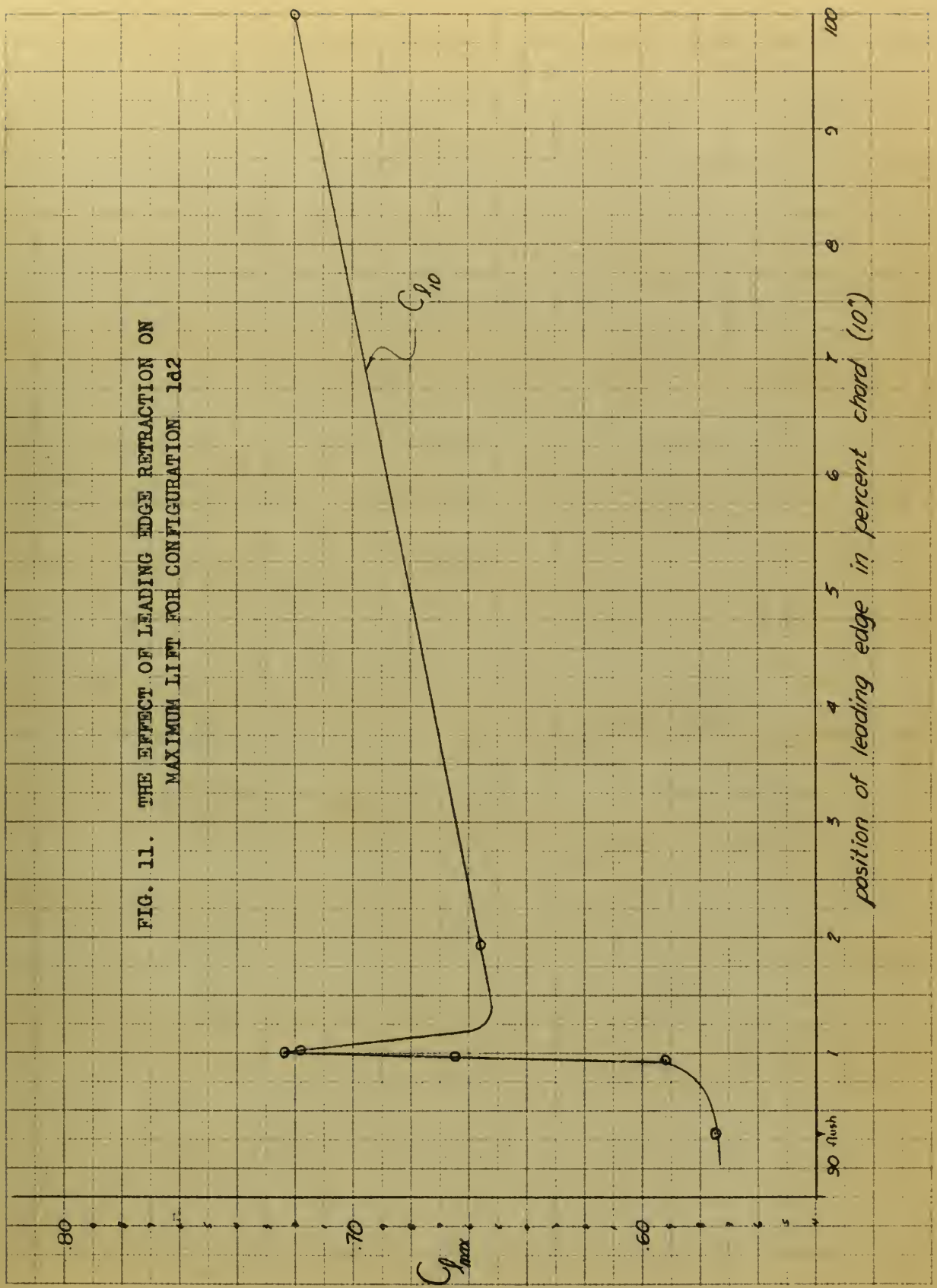
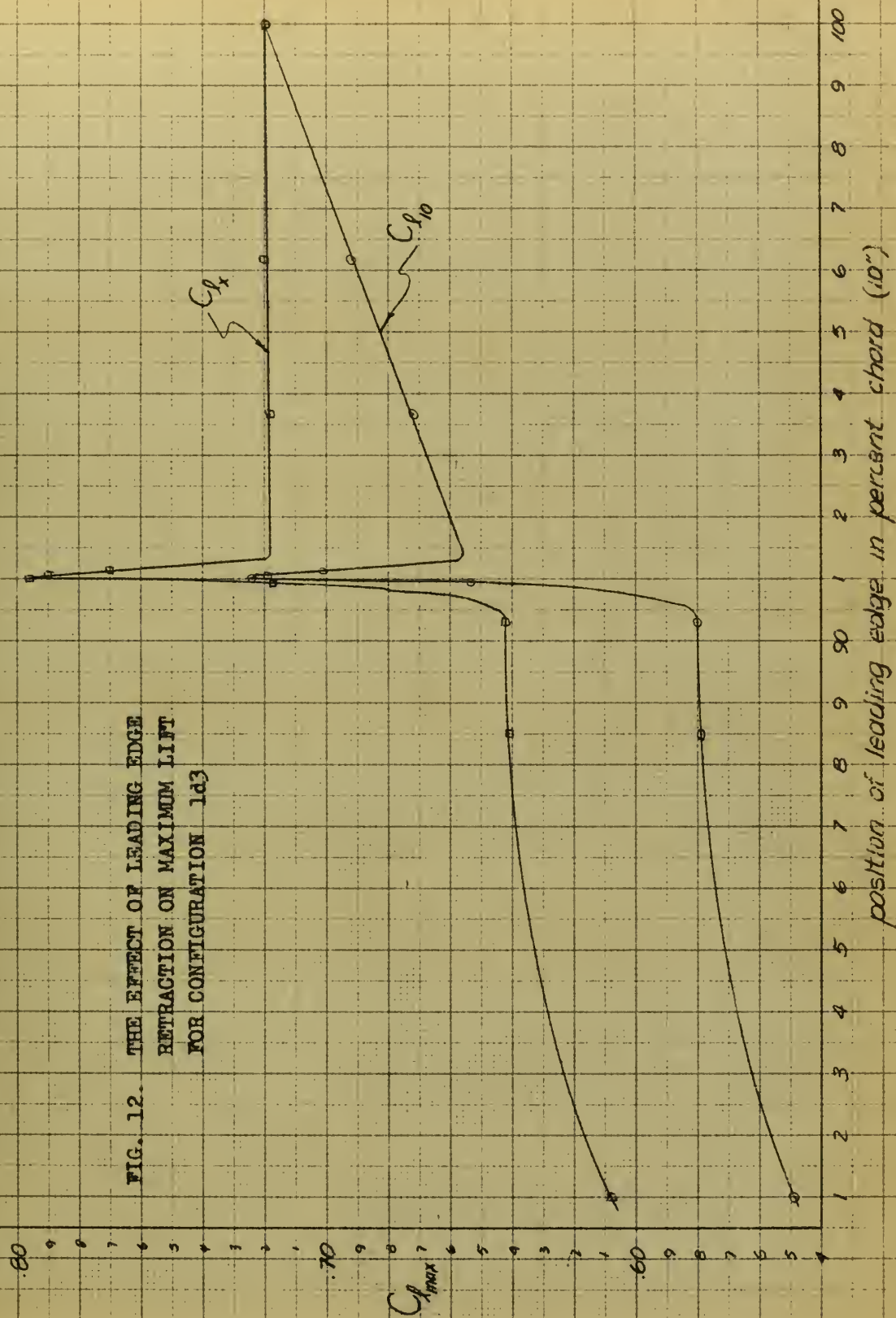


FIG. 12. THE EFFECT OF LEADING EDGE
RETRACTION ON MAXIMUM LIFT
FOR CONFIGURATION 1d3



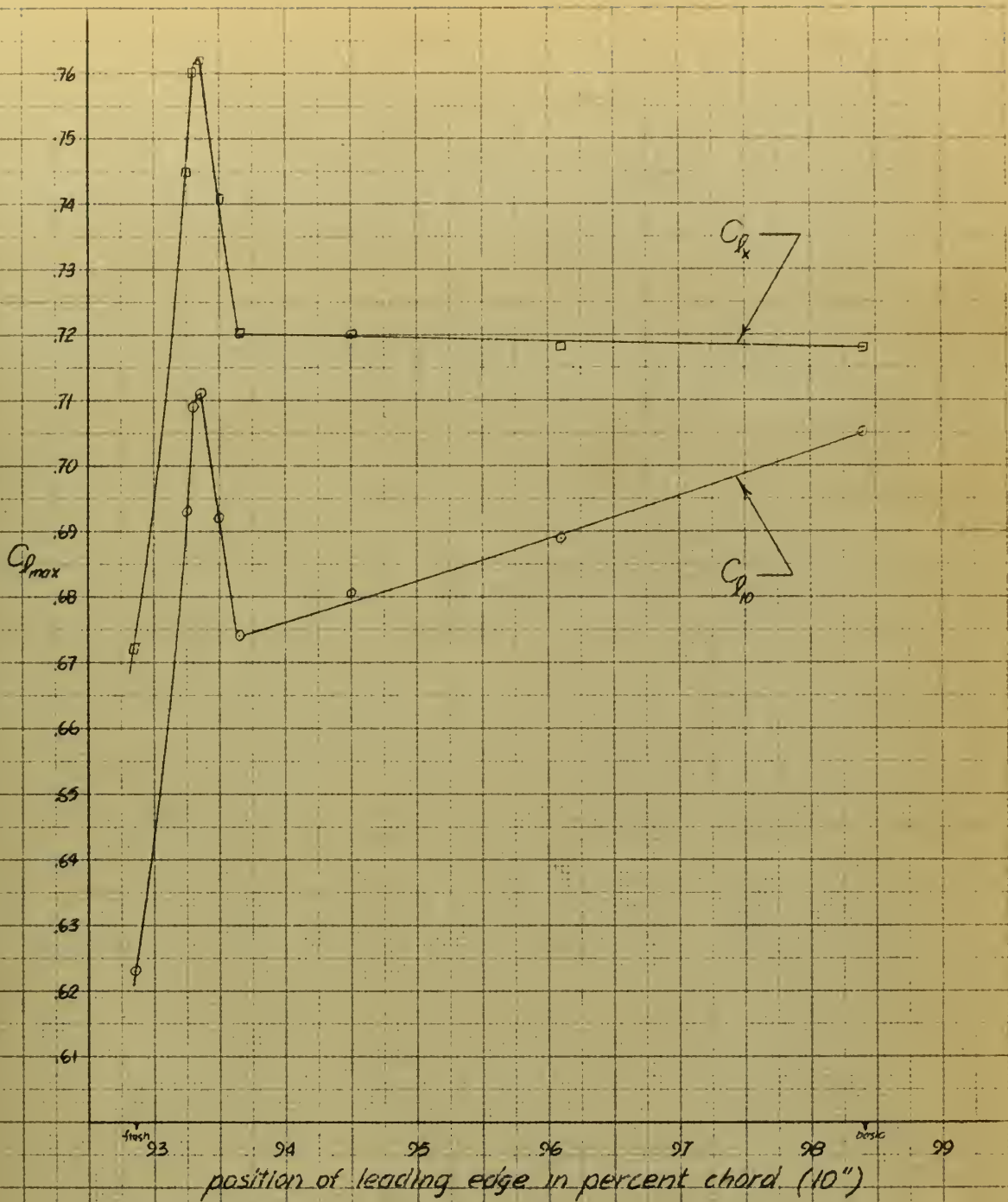


FIG. 13. THE EFFECT OF LEADING EDGE RETRACTION ON MAXIMUM LIFT FOR CONFIGURATION 23

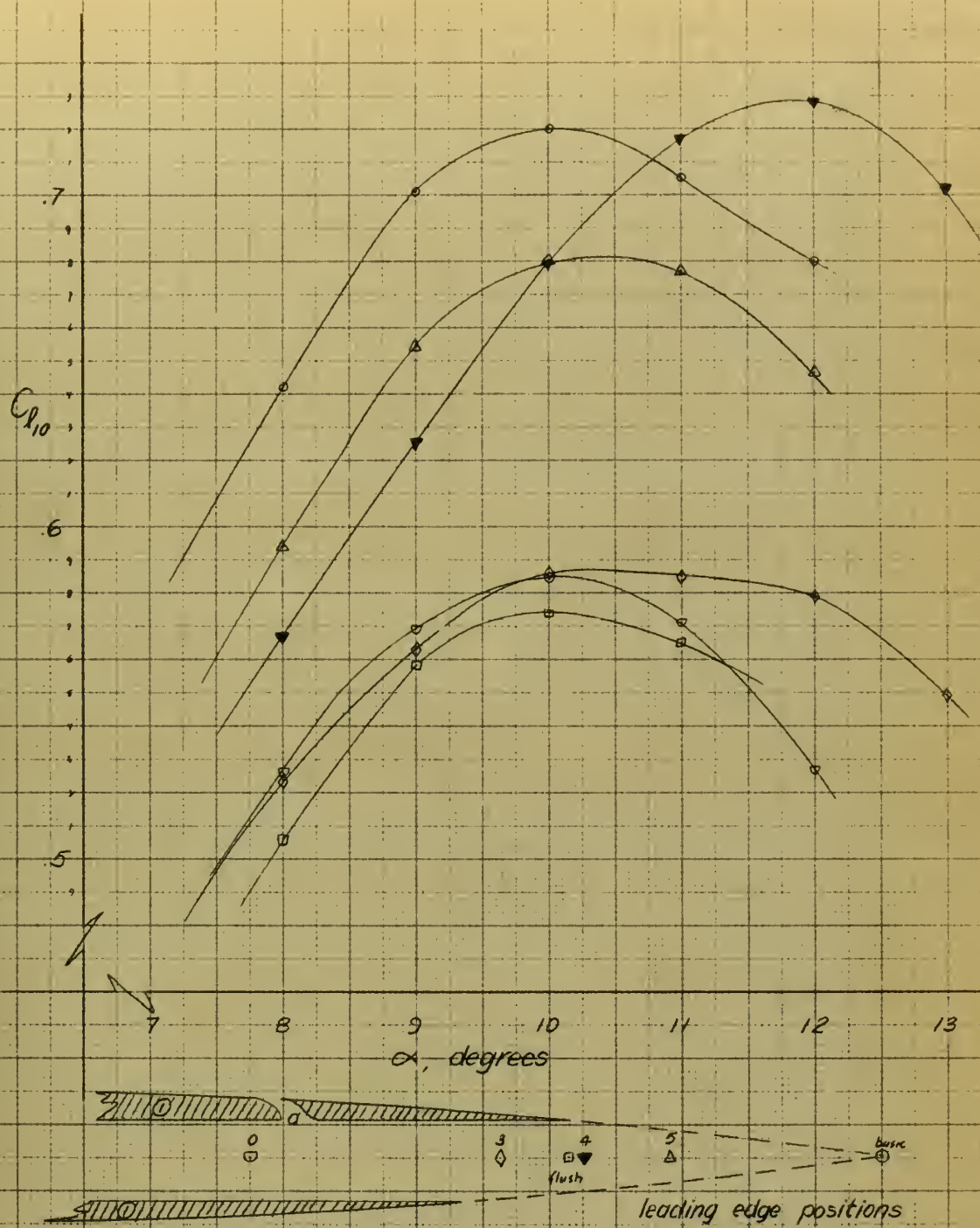


FIG. 14. C_{L10} vs. α FOR CONFIGURATION 1a1

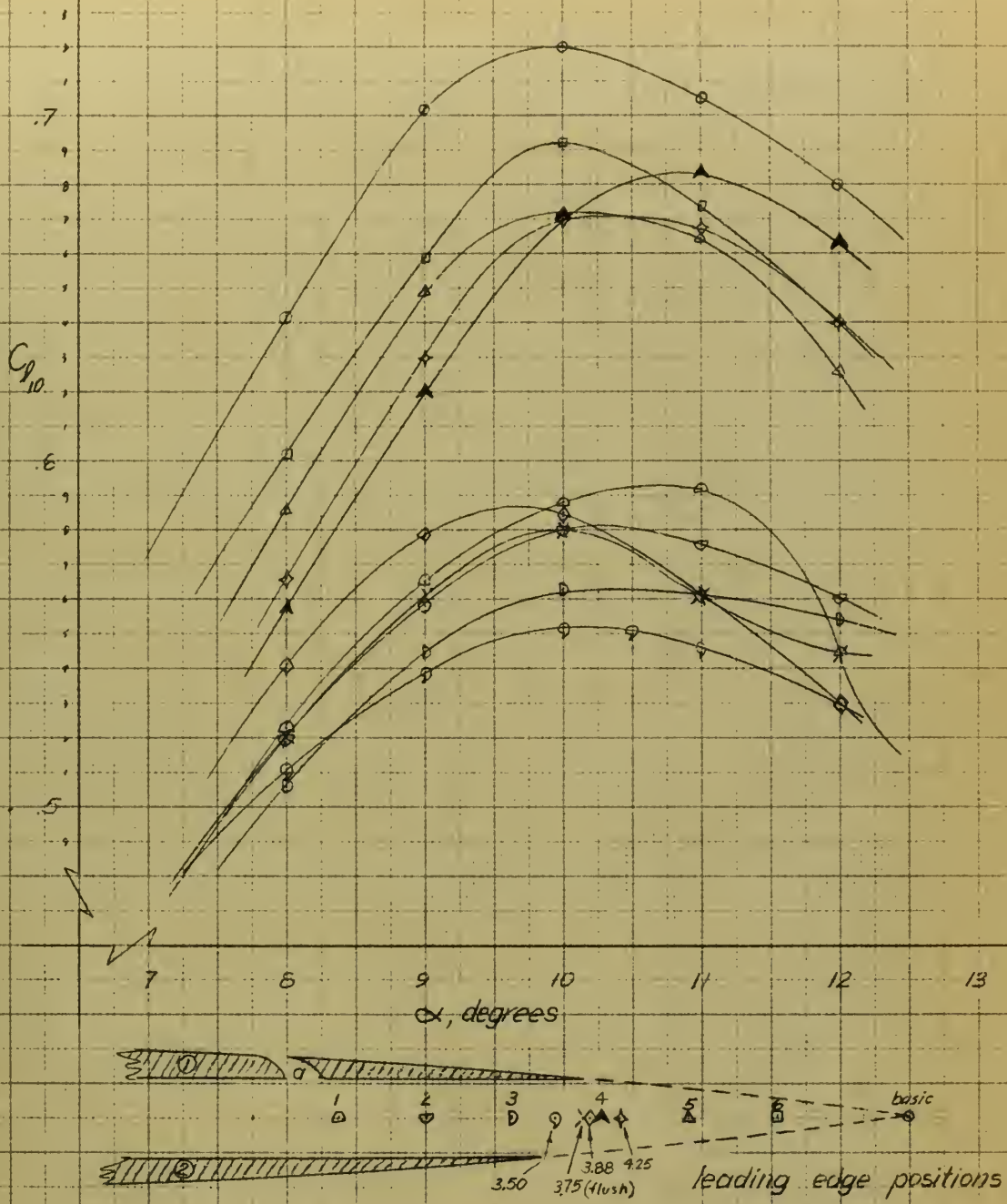


FIG. 15. C_{D10} vs. α FOR CONFIGURATION 1a2

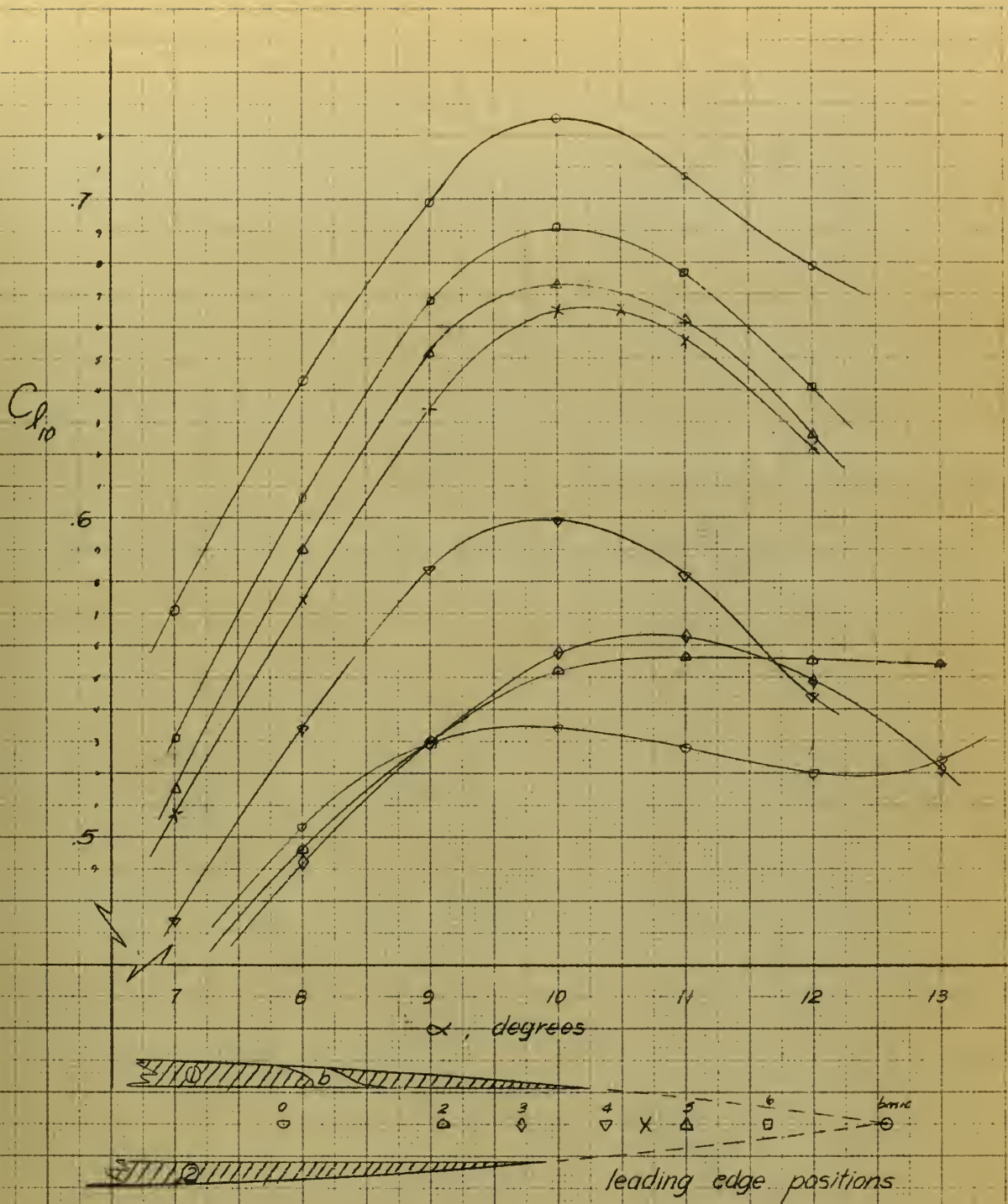


FIG. 16. C_{l10} vs. α FOR CONFIGURATION 1b2

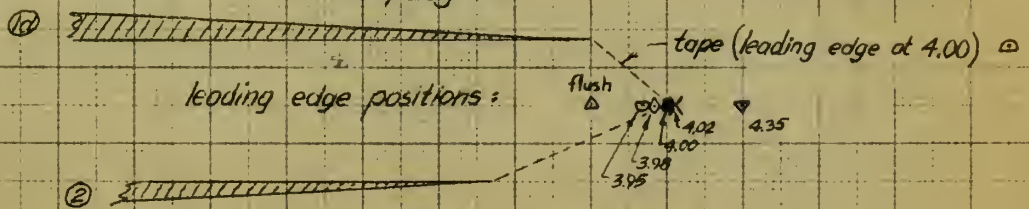
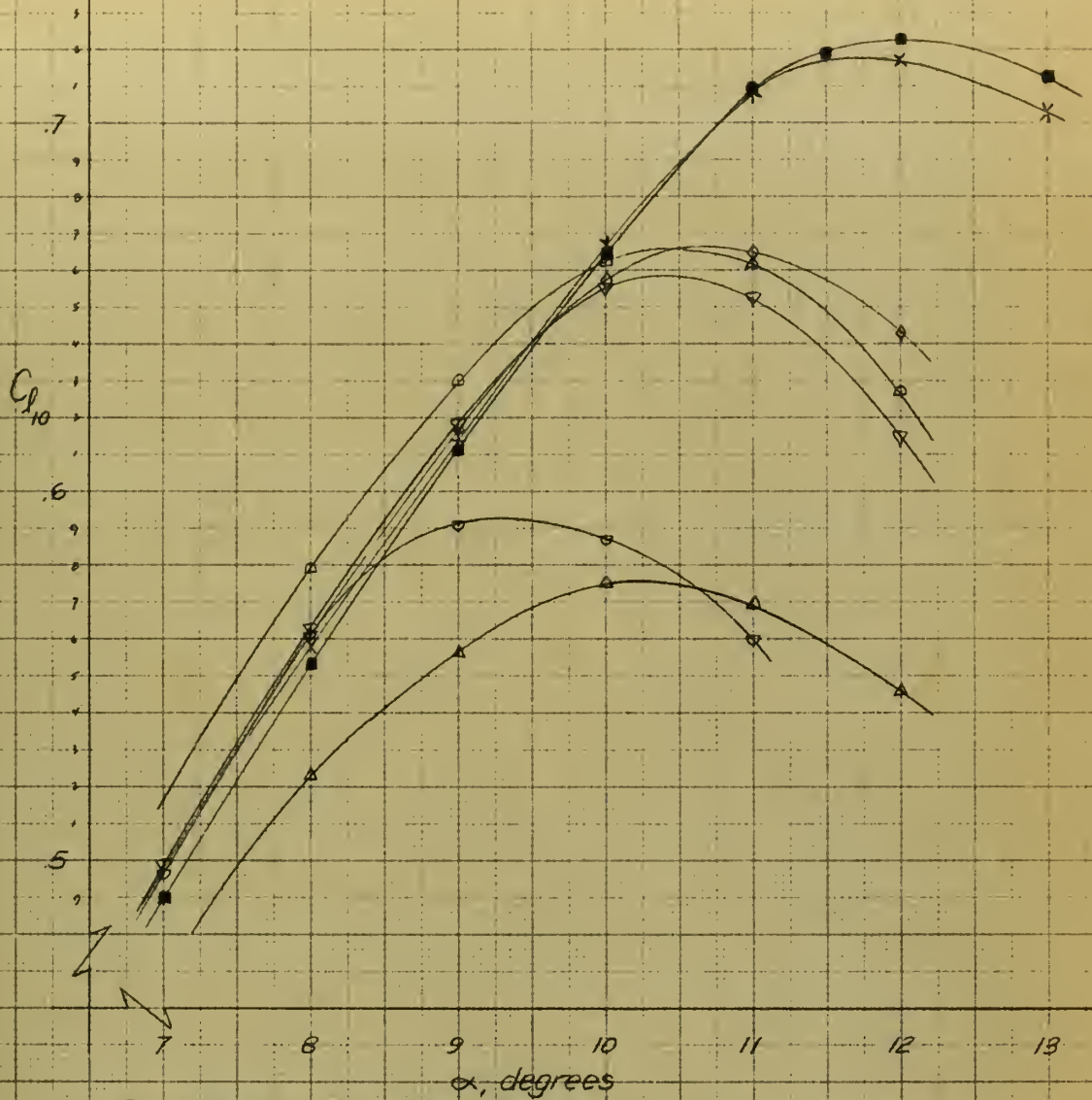


FIG. 17. C_{l10} vs. α FOR CONFIGURATION 1d2

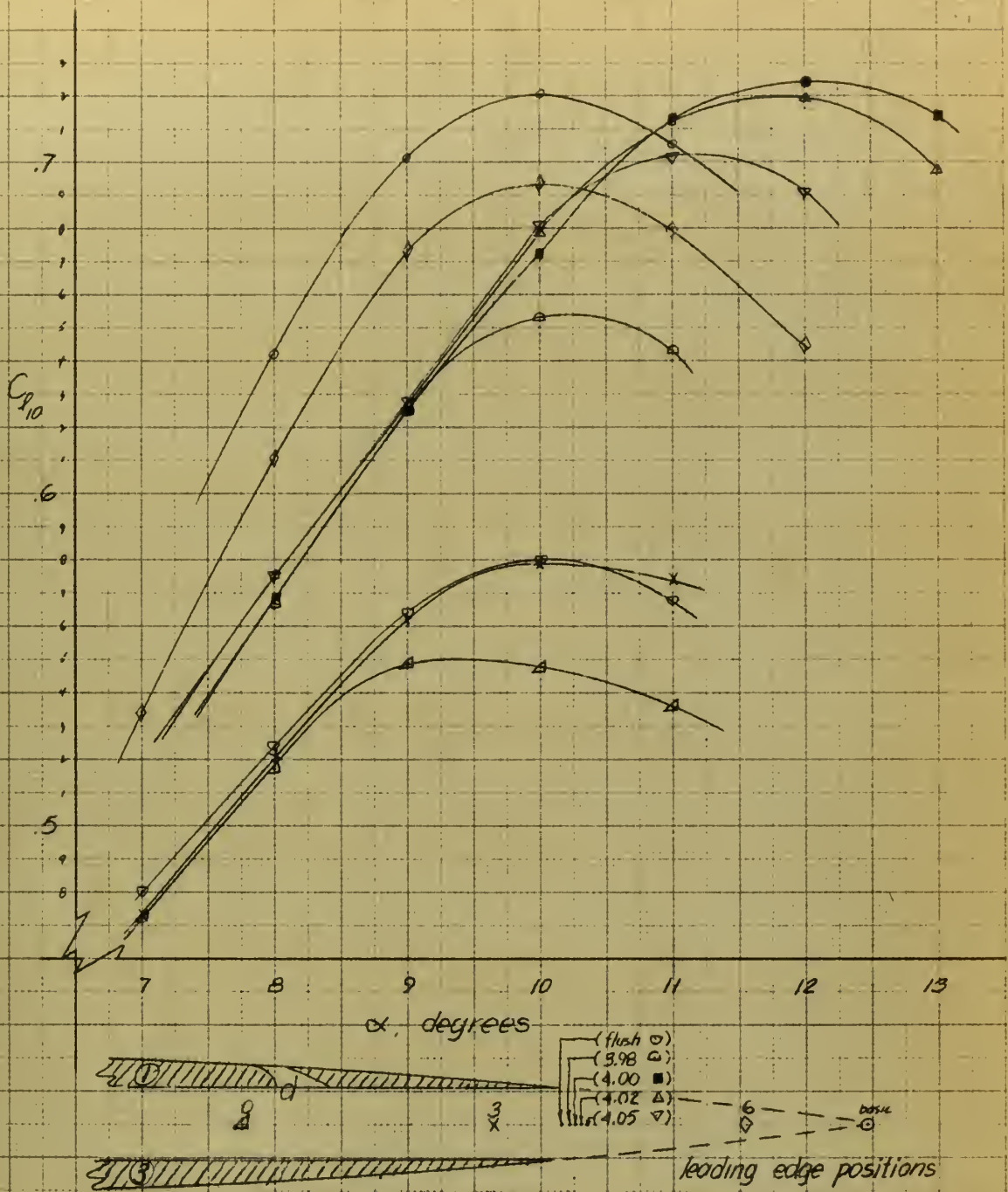
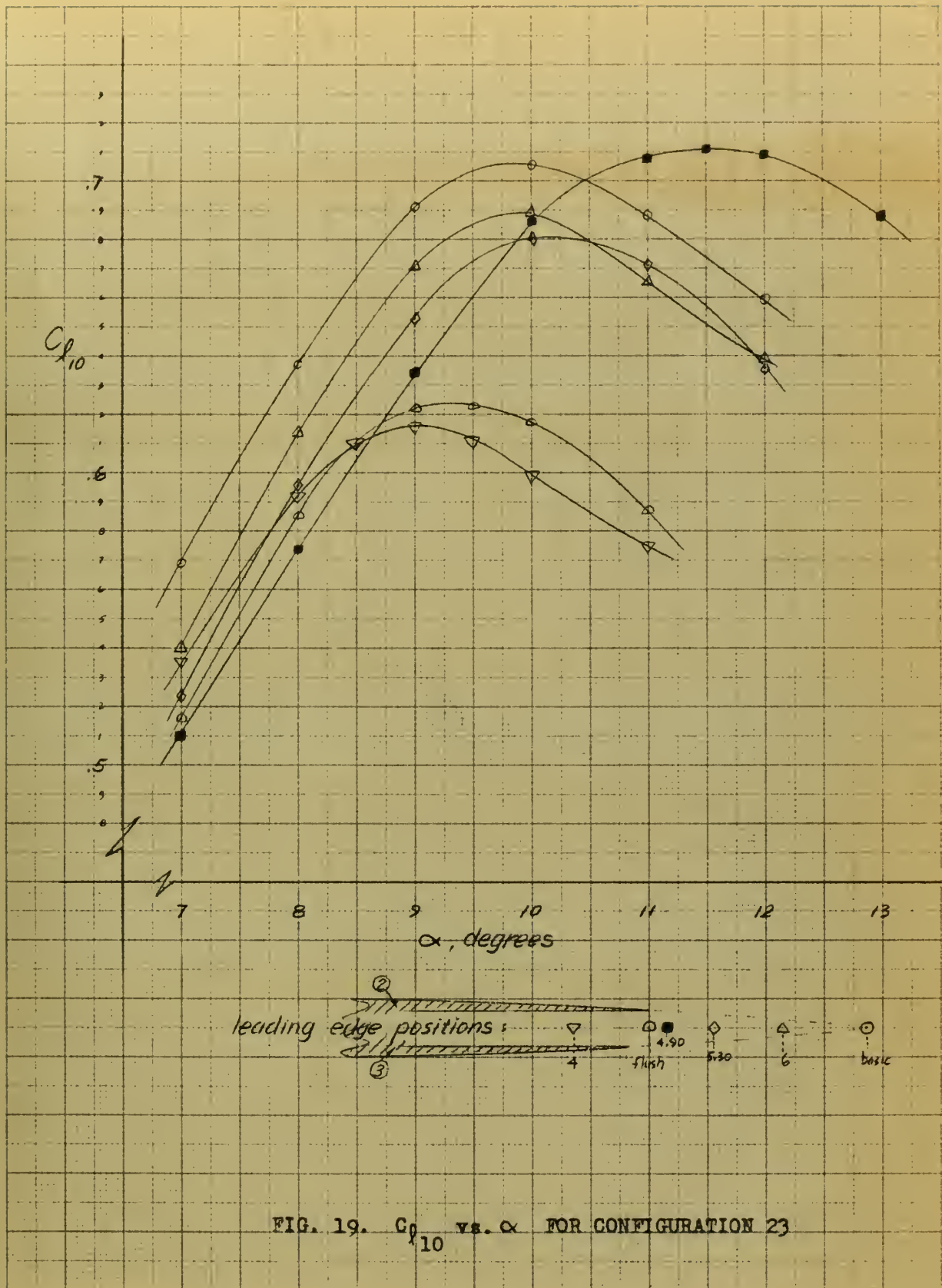


FIG. 18. C_{p10} vs. α FOR CONFIGURATION 1d3



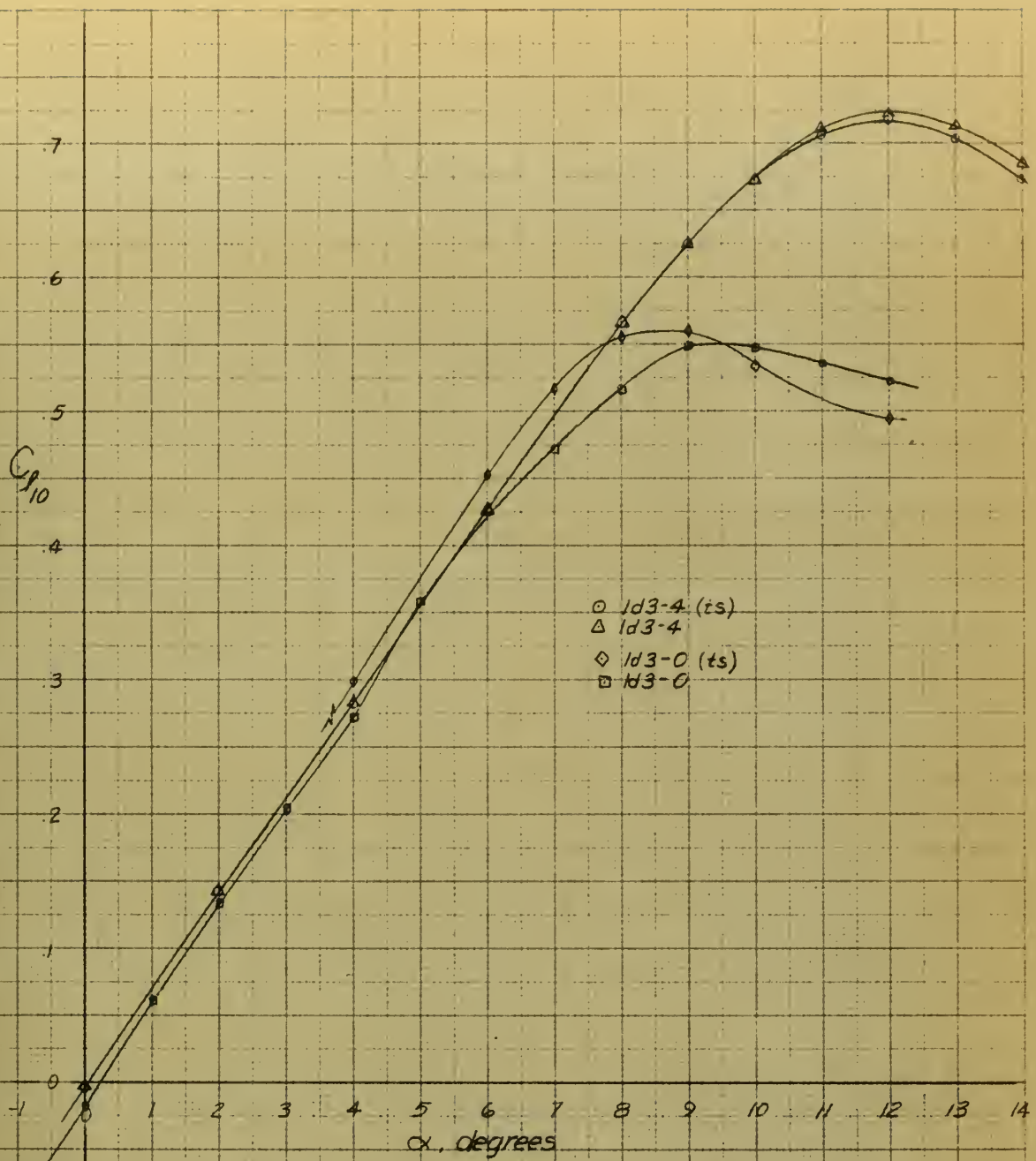


FIG. 20. SLOT EFFECTIVENESS FOR CONFIGURATIONS 1d3-0 AND 1d3-4

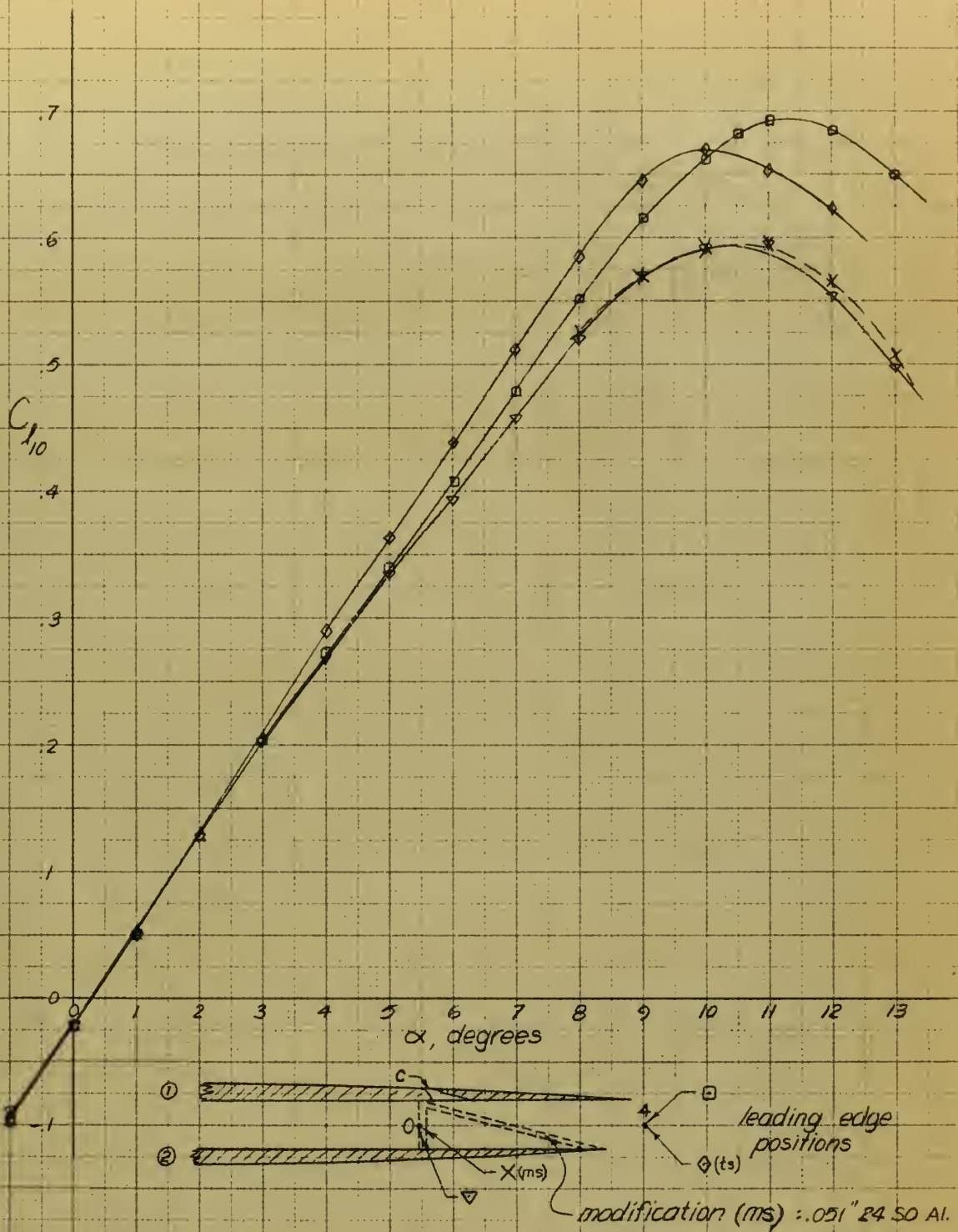
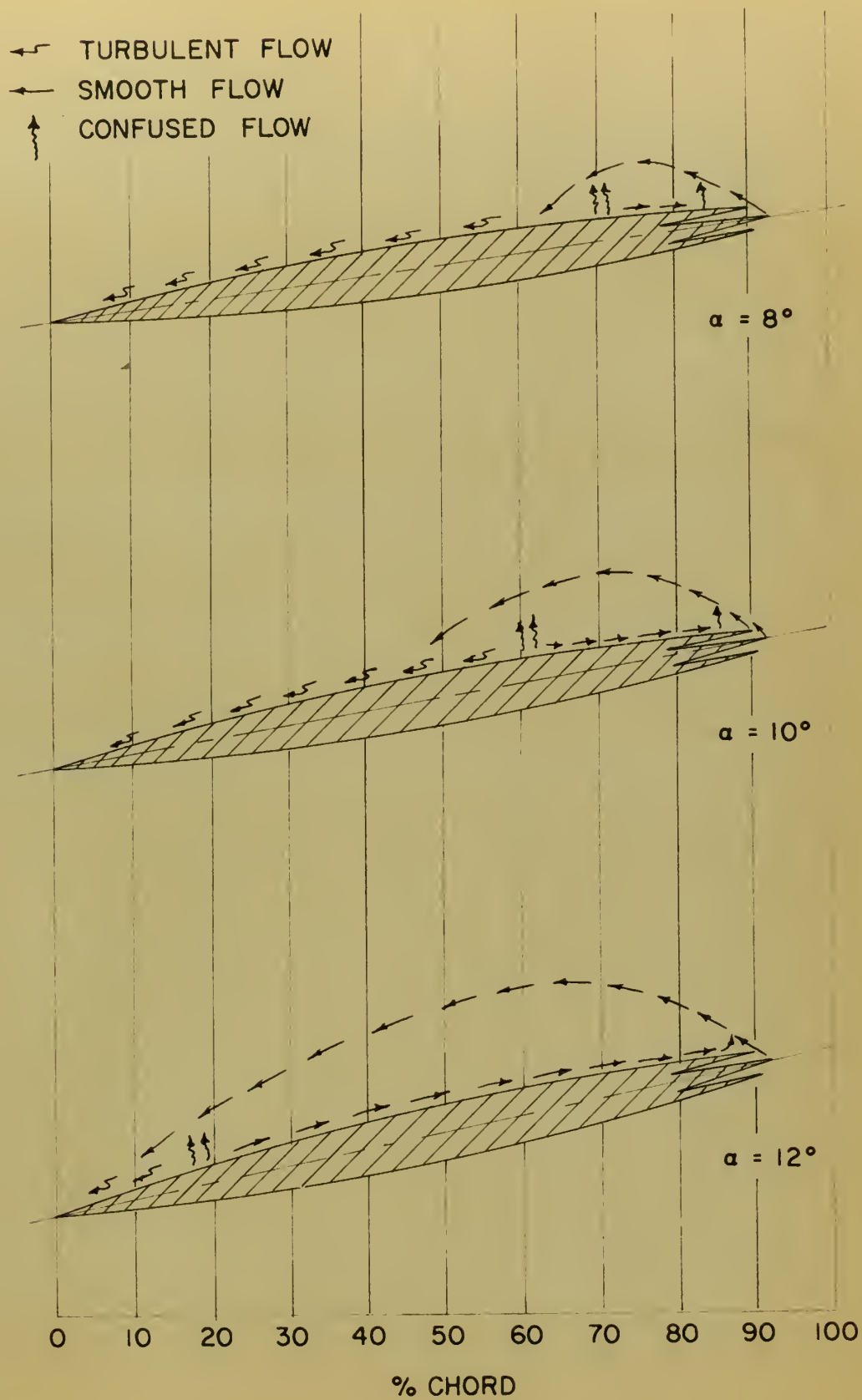


FIG. 21. SLOT EFFECTIVENESS FOR CONFIGURATIONS 1c2-0 AND 1c2-4

FIG. 22 PROBE TUFT SURVEY OF CONFIGURATION 1d3-4



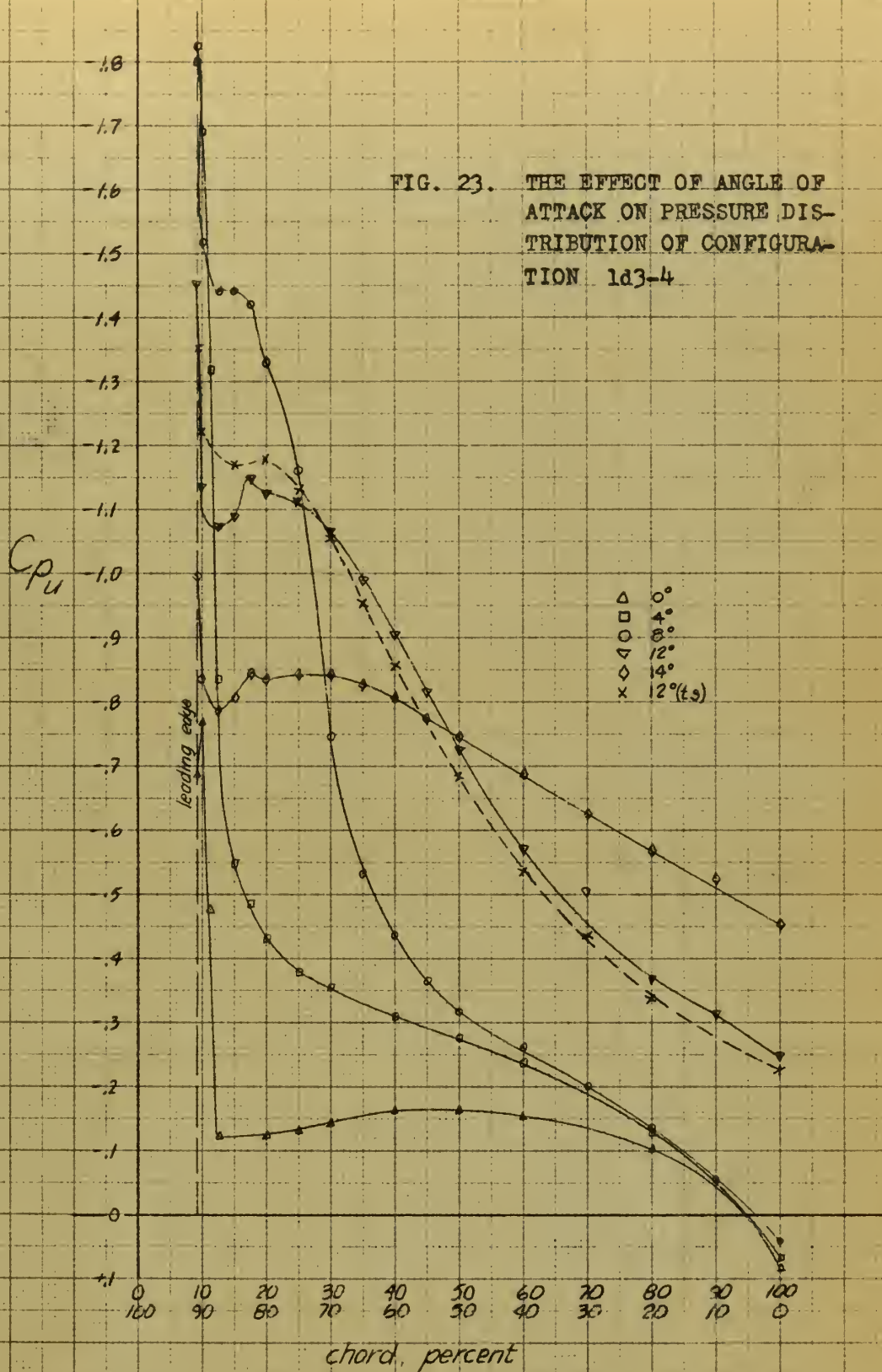


FIG. 24. THE EFFECT OF LEADING EDGE RETRACTION ON THE UPPER SURFACE PRESSURE DISTRIBUTION OF CONFIGURATION 1c2 AT $\alpha = 10^\circ$

C_{pu}

- basic
- △ 1c2-0
- ◐ 1c2-0 (ts)
- ▽ 1c2-4
- ◑ 1c2-4 (ts)

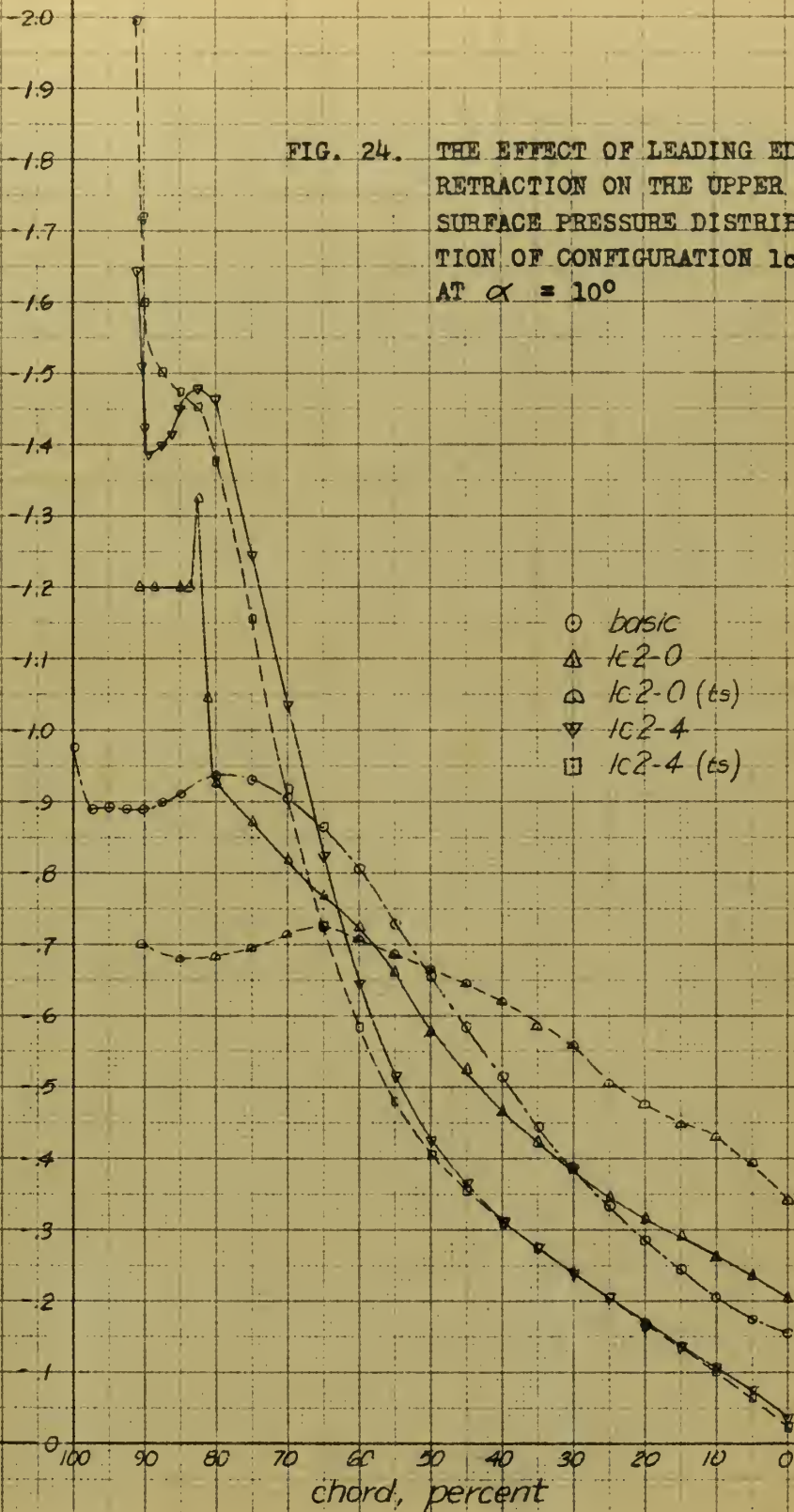
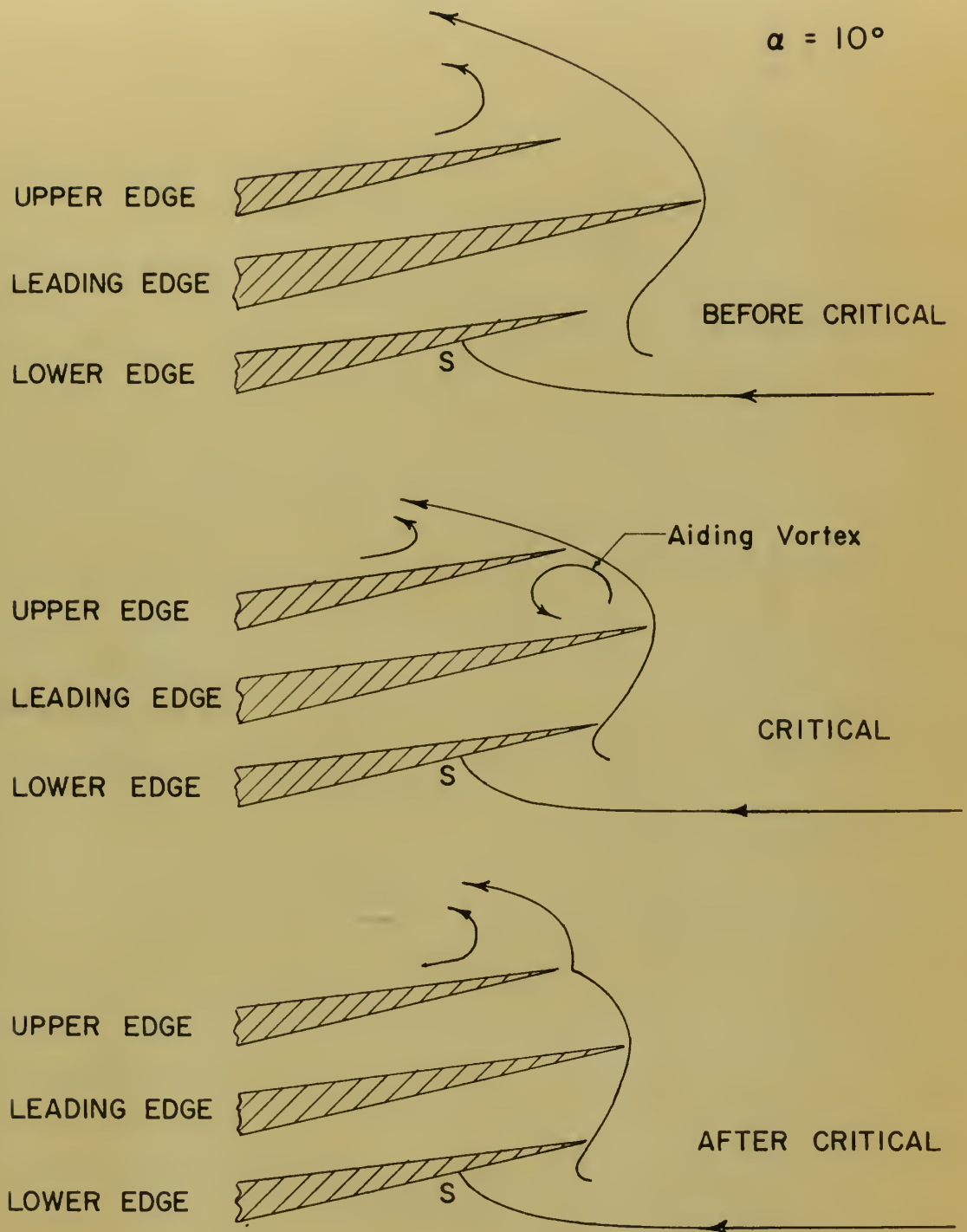


FIG. 25 VORTEX HYPOTHESIS



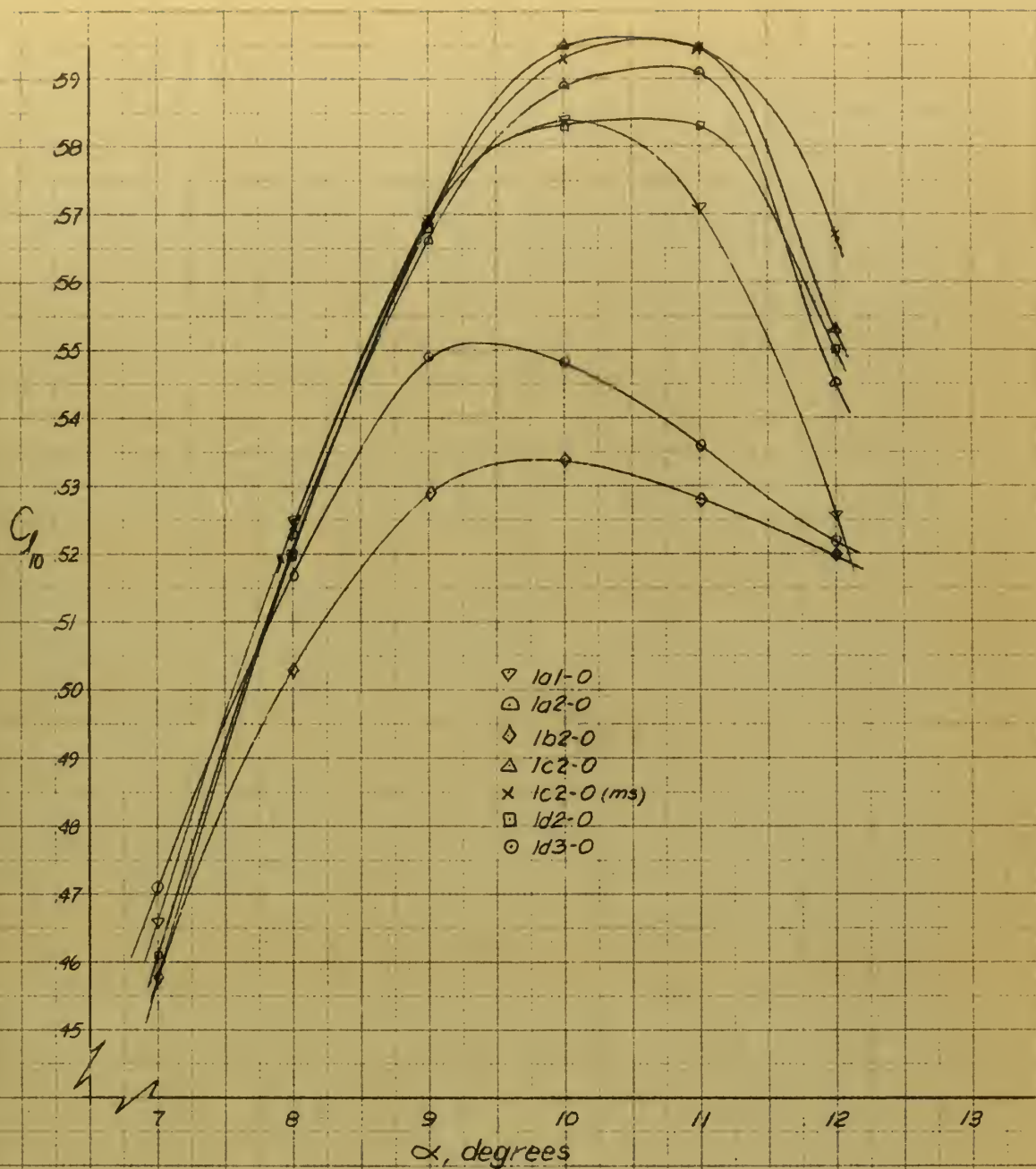


FIG. 26. THE EFFECT OF SLOT SIZE AND CONFIGURATION AT THE FULLY RETRACTED POSITION

D663

28935

Doss

Leading edge retraction
as a high lift device.

D6

D663

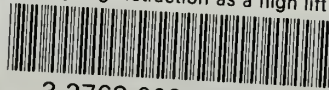
28935

Doss

Leading edge retraction as
a high lift device.

thesD663

Leading edge retraction as a high lift d



3 2768 002 00619 9

DUDLEY KNOX LIBRARY